

The Influence of Strain-Rate History on Stress Strain Diagram of AISI 316 at High Temperature

C. Albertini, M. Montagnani

*Commission of the European Communities, J.R.C. Ispra Establishment, Applied Mechanics Division,
I-21020 Ispra, Italy*

A.M. Eleiche

The American University of Cairo, Dept. of Engineering, P.O. Box 2511, Cairo, Egypt

Abstract

Strain rate jump tests over six orders of magnitude, from 10^3 s^{-1} to 10^{-3} s^{-1} , at temperatures from ambient to 650°C , have been performed using a modified tensile Hopkinson bar, in order to investigate the effects of the strain and strain rate history on the stress-strain characteristics of the austenitic stainless steel AISI 316. Strain ageing effects have been observed, the magnitude of which depends on prestrain values and on temperature.

Introduction

In previous papers, Albertini, Montagnani [1,2], Eleiche, Albertini, Montagnani [3] have reported the calibration of the constitutive equation models proposed by Perzyna [4] and Bodner [5], which correlate stress-strain and strain rate, for the austenitic stainless steel AISI 316L and 316H. The calibration of the different parameters of these models was performed by least-square fitting of the stress-strain curves obtained by tensile tests performed at constant strain rate in the range of $\dot{\epsilon}$ between 10^{-3} s^{-1} and 10^3 s^{-1} , at ambient and high temperatures (400°C , 550°C). By this procedure the calibrated models were able to reproduce the experimental results with an average scatter of $\sim 5\%$. Because such constitutive models should help in analysing the effects of hypothetical accidents of an explosive nature, giving rise to complicated loading patterns, the effects of the strain and strain rate history on the stress-strain curves should be investigated in order to determine the extent of validity of the calibrated constitutive models.

It is the aim of this paper to present the results obtained by prestraining under dynamic conditions specimens of AISI 316H, followed by unloading and successively straining at slow strain rate up to fracture. The inverse procedure, quasi-static prestraining, unloading and dynamic straining up to fracture, was also performed, Eleiche, Albertini, Montagnani [6]. The results obtained will be discussed from the point of view of their impact on the constitutive equations and on the possible modifications which should be introduced in such models. The important modifications of the Hopkinson bar which have been applied in order to perform correct jump tensile experiments, will be presented.

Experimental Procedure

Apparatus

The present series of tests consisted of interrupting the dynamic loading of tensile

specimens after some uniform plastic straining, unloading, then quasi-static reloading up to fracture. The prestraining was performed at a nominal strain rate of $\sim 500 \text{ s}^{-1}$ on a split Hopkinson tension bar. The basics of the technique, as well as its advantages and limitations have been treated extensively in the past, and recently included in two interesting reviews, Lindholm, Nicholas [7,8]. The apparatus (Fig. 2) is a slight modification of the classical design, in order to incorporate a prestressed-bar loading device. Mechanical energy introduced at one end of the system, by means of a hydraulic actuator, is stored in a portion of the input bar, while it is blocked off from the remainder of the system by means of an intermediate brittle piece of known ultimate resistance. With increasing pumping of energy, this piece finally fractures, thus releasing the elastic stored energy and causing a tensile wave to propagate down the remainder of the input bar, test specimen and output bar. This loading wave is nearly rectangular, and characterized by a short rise time of the order of 25 μs and a constant amplitude and long duration thereafter, in proportion with the prestored load and the length of the prestressed bar, respectively. The input and output bars are both instrumented, at stations equally distant from the specimen, with strain gauges, to obtain on an oscilloscope the stress history of the wave before and after its passage through the specimen. Design considerations and complete description and performance of the apparatus are presented in detail elsewhere, Albertini, Montagnani [9].

To carry out the dynamic prestraining tests we have had to modify further the Hopkinson apparatus. Now we can stop the dynamic tests at a given state of deformation, so that the waves reflected along the bar do not induce further, unwanted, deformations in the sample. We thus proceeded as follows: first of all the length of the preloading bar was reduced to the minimum necessary to obtain an impulse which was just sufficiently long to reach the desired deformation rate. This was, however, not sufficient as the waves reflected at the two ends of the bar induced compression waves which deformed the specimen by buckling instability. The diagram obtained can be seen in Fig. 1. One may note the reflected large magnitude compression waves which cause the undesired deformation of the sample. For an analysis of the reflection phenomena which are obtained, see also the diagram of Fig. 2.

Another bar was thus added, after the transmission bar, downstream of the sample. This bar was linked with the previous one by a device which has already been used as a sharpener [9] which can transmit a tension wave but not a compression wave. The result obtained can be seen in Fig. 3. One notes that the reflected compression impulse has practically disappeared. There is, however, a tension impulse which is the result of the reflection of the distension wave which is transmitted, once the clamp is broken, to the end of the prestress bar. This wave has the effect of a compression wave and is reflected to the end of the prestress bar as a new tension wave, which can induce a new deformation in the sample, because of its high intensity.

A further bar has thus been added, suspended by two wires, and placed in contact with the end of the prestress bar. It acts as a ballistic pendulum, capturing the impulse generated by the distension wave (a compression impulse), and transporting it away from the prestress bar by pendulum motion, which cuts the contact with the prestress bar.

The results obtained, which are completely satisfactory for our tests, can be seen in Fig. 4. In this one sees the disappearance of the reflected tension wave. The small reflected compression peak which is still present does not induce further deformations in the sample because its intensity is small. Fig. 5 represents schematically the whole set of waves which

are reflected and transmitted with the final device described above.

Once the desired dynamic predeformation was carried out with the Hopkinson bar equipped with the modifications described above, the specimens of the material under examination were deformed up to rupture with a normal Hounsfield tensometer at a strain rate of $\sim 0.004 \text{ s}^{-1}$ recording on paper the load applied and the total displacement of the cross head.

Specimens

The test material was AISI type 316 (nuclear grade H) stainless steel (JRC reference material), supplied by Uddeholm in Sweden in the form of 50 mm thick hot-rolled plate. The chemical composition (in wt%) was: 16.9 Cr, 12.4 Ni, 1.65 Mn, 2.45 Mo, 0.05 C, 0.35 Si, 0.008 S, 0.020 P, 0.023 Co, 0.001 B, 0.082 N and 66.066 (balance) Fe. All specimens were cut in the rolling direction from this plate, and were not subjected to any post-machining heat treatment. No difference in characteristics was found between specimens taken from the outer or the inner layer of the plate.

The specimen has a short gauge length ($\sim 8 \text{ mm}$) with 3 mm diameter, similar to that used by other investigators, Harding, Hauser [10,11], developed as required by the Hopkinson bar principle such as to achieve homogeneous stress distribution in the specimen by successive reflections of the elastic-plastic waves travelling along the specimen itself.

Testing procedure. The procedure in each test was quite straightforward. Before testing any given specimen, its dimensions, particularly its diameter and gauge length, were carefully measured. It was then loaded in the Hopkinson bar up to a total strain within the plastic range, unloaded, carefully removed from the set-up and remeasured. Finally, it was mounted in the Hounsfield tensometer and reloaded to fracture. This whole procedure did not take more than 20 minutes, on average.

Data reduction. After having dynamically prestrained the specimens using the Hopkinson bar within the validity of some simplifying assumptions, average values of engineering stress (σ_e), strain (ϵ_e) and strain rate ($\dot{\epsilon}_e$) in the specimen can be calculated from the relationship [7]:

$$\begin{aligned} \dot{\epsilon}_e &= \frac{2c_b}{L_0} \epsilon^R \\ \epsilon_e &= \frac{2c_b}{L_0} \int_0^t \epsilon^R dt \\ \sigma_e &= E \frac{A_b}{A_0} \epsilon^T \end{aligned} \tag{1}$$

where ϵ^R and ϵ^T are the reflected and transmitted strain waves measured on the input and output bar, respectively, E is the Young's modulus, A_b is the cross-sectional area and c_b is the wave velocity of the elastic bars. L_0 and A_0 are the gauge length and cross-sectional area, respectively, of the specimen prior to the dynamic test.

Corresponding true stresses and true strains were then calculated, and the dynamic curve plotted. During the successive quasi-static straining up to fracture on the Hounsfield tensometer, by proper scaling, load and displacement records obtained in any test were calibrated and cross-plotted to provide an engineering stress-strain curve for the specimen, due account

being taken of the elastic deformation of the system. For more accurate description of the behaviour, this was then translated into a true stress/true strain curve, which was plotted with the origin displaced on the strain axis by a value equal to the dynamic plastic pre-strain. The reduction procedure of the experimental data is described in ref. [9]. Each monotonic curve of Figs. 6 to 12 is the average of 3:4 specimen tests while the jump curves are the result of a single test for each value of prestrain.

Results and Discussion

The results obtained at the ambient temperature and at 100, 200, 300, 400, 550 and 650°C are presented in Figs. 6 to 12. On each of these diagrams the curves A and B represent the stress-strain relationship obtained by monotonic tensile tests at strain rates of $\sim 0.004 \text{ s}^{-1}$ and $\sim 500 \text{ s}^{-1}$, respectively. The other curves on these diagrams represent the stress-strain relationships obtained by the tensile tests interrupted at different strain levels followed by a strain rate jump. The monotonic curves A and B at all temperatures show an increase of the flow stress at a given strain with increasing strain rate; this increase is highest at ambient temperature and practically disappears at 650°C.

The general trend of the quasi-static reloading curve is complex and presumably governed by strain ageing phenomena (Baird [12], Klepaczko, Duffy [18]), which depend on dynamic pre-strain and on temperature, except at 100°C where the quasi-static reloading curve does not differ from the monotonic stress-strain curve. The dependence of strain ageing on dynamic prestrain is shown by the quasi-static reloading curve at ambient temperature where one observed an increasing static strain ageing (ageing after straining) effect with increasing dynamic prestrain, the same dependence being observed at the temperatures of 300, 400 and 550°C.

Furthermore, the quasi-static reloading curves at the temperatures of 400, 550 and 650°C also show phenomena of dynamic strain ageing [12,13] (ageing during straining) manifested by the serrations along the flow curves. The quasi-static reloading curves at the temperatures of 200 and 650°C also show overageing phenomena where the quasi-static reloading curves lie under the monotonic one.

Strain ageing phenomena were also observed on the dynamic reloading curve obtained at high temperatures (300, 400, 550, 650°C) [6] after a quasi-static prestraining.

It is not intended to discuss here the complicated physical and microstructural phenomena causing strain ageing phenomena. That topic has been dealt with in other papers [12,13, 14,15,16,17]. In this paper we wish to stress the fact that strain and strain rate histories have an effect on the stress-strain relationships. This effect becomes greater with pre-strain and temperature. In particular the results presented here and in [6], permit us to affirm that the constitutive models calibrated on the monotonic stress-strain relationships determined at constant strain rate are able to represent the material behaviour with a reasonable agreement for values of total plastic strain up to 20% and for temperatures from ambient to 200°C, independent of strain and strain rate histories, therefore assuming the significance of an equation of state within these limits. At higher values of total plastic strain and temperatures, strain ageing phenomena must be modelled and included in the constitutive equation in order to render it able to represent the material behaviour over larger values of total plastic strain and at higher temperatures. Attempts to model the strain ageing phenomenon have already been made [12,13,15,17] and are based on the activation energy

theory, which is consistent with the theoretical development of the Perzyna and Bodner constitutive models. Improvements in the modelling of strain ageing phenomena can be achieved by microstructural observations on a fine scale, performed during and/or after testing, because the current physical interpretations of such phenomena call for interactions between dislocations and interstitials of various natures [12].

Conclusions

An accurate analysis of wave propagation phenomena is necessary in order to perform dynamic prestraining experiments which permit correct loading and deformation measurements of the specimens. The improvements and modifications adopted in the Hopkinson bar experiments have allowed the obtaining of well controlled strain and strain rate histories on specimens of AISI 316H, in order to measure the effects of such histories on the material behaviour. The strain rate jumps performed over six orders of magnitude from 10^3 to 10^{-3} s⁻¹ and from 10^{-3} to 10^3 s⁻¹ revealed strain ageing phenomena which modify the stress-strain characteristics determined with monotonic tensile tests. These modifications are important for strains higher than 20% and at high temperatures. It follows that the constitutive equations calibrated on the monotonic stress-strain curves are reasonably independent of the strain and strain rate histories for total plastic strain less than 20% and temperatures from ambient up to 200°C. For higher plastic strain and temperatures the constitutive equations must be able to model the effects of strain ageing.

Acknowledgements

The authors wish to thank Messrs. A. Pachera and M. Forlani for setting up the experimental apparatus and for performing the tests.

References

- [1] ALBERTINI, C., CENERINI, R., CURIONI, S., MONTAGNANI, M., "Dynamic mechanical properties of austenitic stainless steels - fitting of experimental data on constitutive equations", VII SMIRT, August 1983, Chicago, paper L 2/4.
- [2] ALBERTINI, C., CENERINI, R., CURIONI, S., GRIFFITHS, L.J., MONTAGNANI, M., "Constitutive equations of steels in dynamics as a function of temperature and strain rate - techniques and results", Conf. on Dynamical Mechanical Properties and Fracture Dynamics of Engineering Materials, Inst. of Physical Metallurgy, Czechoslovak Academy of Sciences, June 1983, Valtice (BRNO).
- [3] ELEICHE, A.M., ALBERTINI, C., MONTAGNANI, M., "The influence of strain rate history on the ambient tensile strength of AISI type 316 stainless steel", High Energy Rate Fabrication 1984, ASME, Book No. H00318.
- [4] PERZYNA, P., PECKERSKI, R.B., "Modified theory of viscoplasticity - physical foundations and identification of material functions for advanced strains", Arch. Mechanics 35, 423-436, 1983.
- [5] BODNER, S.R., PARTOM, Y., "Constitutive equations for elastic-viscoplastic strain hardening materials", J. Appl. Mech. 42, 2, 385-389 (1975).
- [6] ELEICHE, A.M., ALBERTINI, C., MONTAGNANI, M., "Response of AISI type 316 stainless steel to interrupted quasi-static to impact tension at elevated temperature", Proc. of Int. DYMAT 85, Paris.

- [7] LINDHOLM, U.S. (1971) in: *Techniques of Metal Research, Vol.V - Measurement of Mechanical Properties, Part 1*, Interscience Publishers, N.Y., 199-271.
- [8] NICHOLAS, T. (1983) in: *Impact Dynamics*, Wiley, New York, 277-332.
- [9] ALBERTINI, C., MONTAGNANI, M. (1977) "Dynamic material properties of several steels for fast breeder reactor safety analysis", Tech. Rep. No. EUR 5787EN, JRC-Ispra, Italy.
- [10] HARDING, J., WOOD, E.D., CAMPBELL, J.D. (1960) *J. Mech. Eng. Sci.*, 2, 88-93.
- [11] HAUSER, F.E. (1966) *Experimental Mechanics*, 6, 395-400.
- [12] BAIRD, J.D., "The effects of strain-ageing due to interstitial solutes on the mechanical properties of metals", *Metallurgical Reviews*, 16, 1971, 1.
- [13] CHAKRAVARTTY, J.K., WADEKAR, S.L., SINHA, T.K., ASUNDI, M.K., "Dynamic strain-ageing of A 203 D nuclear structural steel", *J. of Nuclear Materials*, 119 (1983) 51-58.
- [14] CERNY, V., CADEK, J., "Creep, the Portevin-Le Chatelier effect and dynamic strain ageing in 18Cr-12Ni and 17Cr-13Ni-2.5Mo stainless steels", *Materials Science and Engineering*, 66 (1984) 89-96.
- [15] KANEAKI TSUZAKI, TAKASHI HORI, TADASLU MAKI, IMAO TAMURA, "Dynamic strain ageing during fatigue deformation in type 304 austenitic stainless steel", *Material Science and Engineering*, 61 (1983) 247-260.
- [16] SAHA, G.G., MCCORMICK, P.G., RAMA RAO, P., "Portevin-Le Chatelier effect in an Al-Mn alloy I: serration characteristics", *Materials Science and Engineering*, 62 (1984) 187-196.
- [17] CLOUGH, W.R., JACKMAN, L.A., ANDREW, Y.G., "Dynamic strain ageing and the Charpy specimen behaviour of annealed 4340 steel", *J. of Basic Eng.*, March 1968, 13-20.
- [18] KLEPACZKO, J., DUFFY, J., "History effects in polycrystalline BCC metals and steel subjected to rapid changes in strain rate and temperature", *Arch. Mech.* 34, 1982, 419-436.



FIG. 1.-
TEST PERFORMED WITH PRESTRESSED BAR,
1550 mm LONG, WITHOUT ADDITIONAL BARS

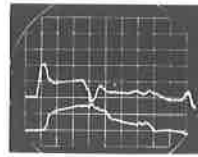


FIG. 4.-
TEST PERFORMED WITH THE FURTHER ADDITION OF
A BAR AS A BALLISTIC PENDULUM ON THE MOUNTAIN
SIDE OF THE PRESTRESSED BAR

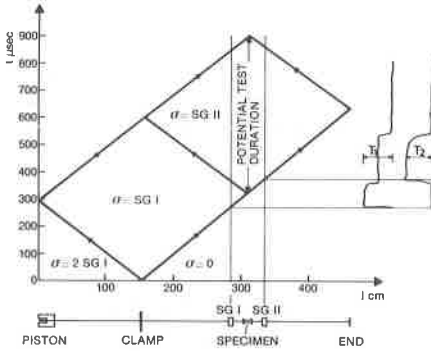


FIG. 2.- WAVE TRANSMISSION AND REFLECTION WITH A
SHORT PRESTRESSED BAR

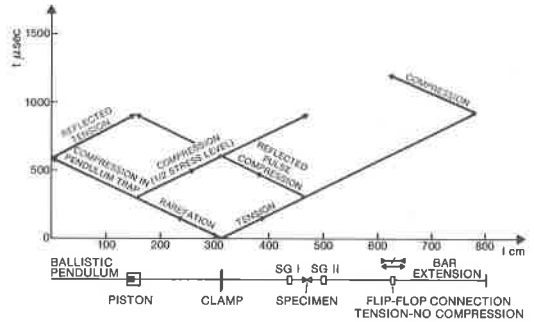


FIG. 5.- WAVE TRANSMISSION AND REFLECTION WITH THE
ADDITION OF AN EXTENSION BAR AND A BALLISTIC
PENDULUM

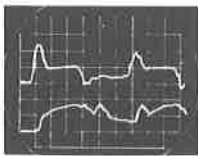


FIG. 3.-
TEST PERFORMED WITH THE ADDITION OF A BAR
ON THE VALLEY SIDE OF THE TRANSMISSION BAR

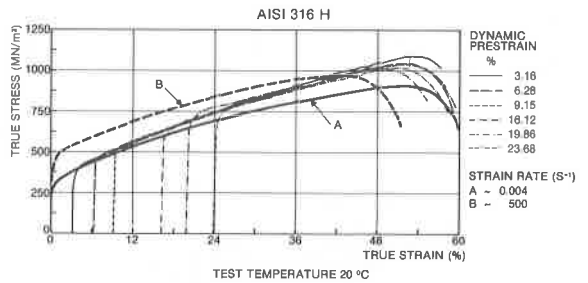


FIG.-6 TENSILE TRUE STRESS-TRUE STRAIN CURVES AT
AMBIENT TEMPERATURE FOR MONOTONIC LOADING
TO FRACTURE AT A STRAIN RATE OF 0.004 S⁻¹
(CURVE A) AND 500 S⁻¹ (CURVE B), AND FOR DYNAMIC
PRESTRAINING FOLLOWED BY QUASI-STATIC
RELOADING TO FRACTURE

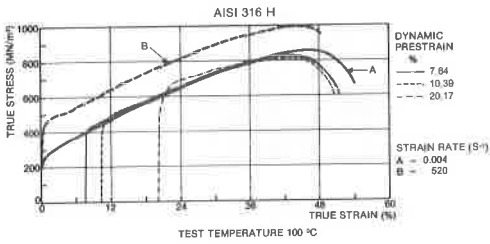


FIG-7 TENSILE TRUE STRESS-TRUE STRAIN CURVES AT 100 °C FOR MONOTONIC LOADING TO FRACTURE AT A STRAIN RATE OF 0.004 S⁻¹ (CURVE A) AND 520 S⁻¹ (CURVE B), AND FOR DYNAMIC PRESTRAINING FOLLOWED BY QUASI-STATIC RELOADING TO FRACTURE

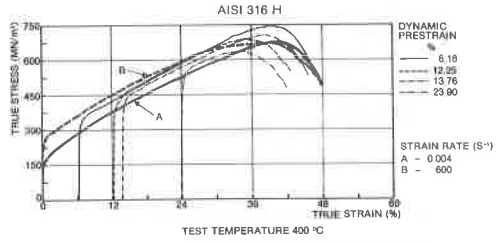


FIG-10 TENSILE TRUE STRESS-TRUE STRAIN CURVES AT 400 °C FOR MONOTONIC LOADING TO FRACTURE AT A STRAIN RATE OF 0.004 S⁻¹ (CURVE A) AND 600 S⁻¹ (CURVE B), AND FOR DYNAMIC PRESTRAINING FOLLOWED BY QUASI-STATIC RELOADING TO FRACTURE

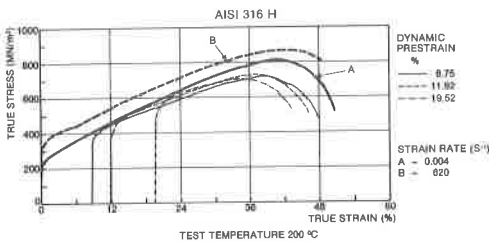


FIG-8 TENSILE TRUE STRESS-TRUE STRAIN CURVES AT 200 °C FOR MONOTONIC LOADING TO FRACTURE AT A STRAIN RATE OF 0.004 S⁻¹ (CURVE A) AND 620 S⁻¹ (CURVE B), AND FOR DYNAMIC PRESTRAINING FOLLOWED BY QUASI-STATIC RELOADING TO FRACTURE

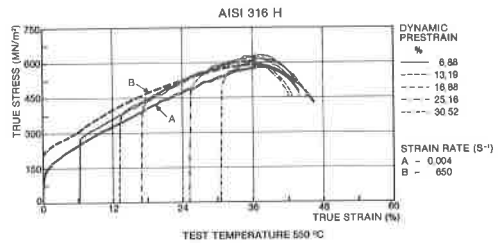


FIG-11 TENSILE TRUE STRESS-TRUE STRAIN CURVES AT 550 °C FOR MONOTONIC LOADING TO FRACTURE AT A STRAIN RATE OF 0.004 S⁻¹ (CURVE A) AND 650 S⁻¹ (CURVE B), AND FOR DYNAMIC PRESTRAINING FOLLOWED BY QUASI-STATIC RELOADING TO FRACTURE

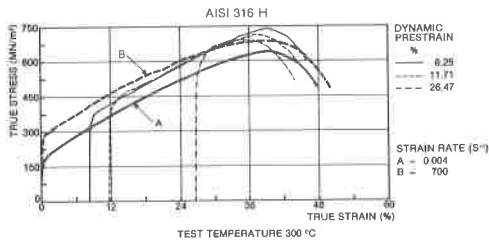


FIG-9 TENSILE TRUE STRESS-TRUE STRAIN CURVES AT 300 °C FOR MONOTONIC LOADING TO FRACTURE AT A STRAIN RATE OF 0.004 S⁻¹ (CURVE A) AND 700 S⁻¹ (CURVE B), AND FOR DYNAMIC PRESTRAINING FOLLOWED BY QUASI-STATIC RELOADING TO FRACTURE

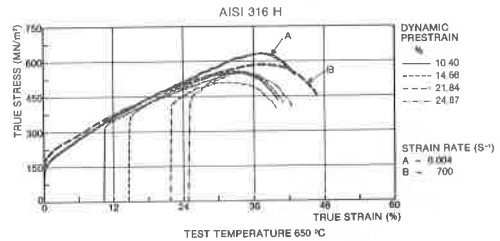


FIG-12 TENSILE TRUE STRESS-TRUE STRAIN CURVES AT 650 °C FOR MONOTONIC LOADING TO FRACTURE AT A STRAIN RATE OF 0.004 S⁻¹ (CURVE A) AND 700 S⁻¹ (CURVE B), AND FOR DYNAMIC PRESTRAINING FOLLOWED BY QUASI-STATIC RELOADING TO FRACTURE